Hindawi
Journal of Chemistry
Volume 2020, Article ID 4156216, 12 pages
https://doi.org/10.1155/2020/4156216

Research Article

Kinetic Modeling Study of the Industrial Sulfur Recovery Process for Operating Condition Optimization

Shan Huang,[1] **Zhaohui Teng**,[1] **Lisheng Zhang**,[2] **Qulan Zhou**,[1] **and Na Li**[1]

[1]*State Key Laboratory of Multiphase Flow in Power Engineering, Xi'an Jiaotong University, Xi'an 710049, China*
[2]*Natural Gas Purification Plant of Puguang Gasfield, Dazhou 636150, China*

Correspondence should be addressed to Qulan Zhou; qlzhou@mail.xjtu.edu.cn

Received 20 March 2020; Accepted 12 May 2020; Published 25 May 2020

Guest Editor: Norbert Miskolczi

Sulfur recovery from acid gas (H_2S and CO_2), which is contained in fresh natural gas, can bring many economic and environmental benefits, and this topic has been studied for years. Finding an optimal operating condition for the factory is of much importance. In this paper, we built a reactor network analysis model with a detailed mechanism to describe and calculate the process in the sulfur recovery unit. This detailed mechanism included 94 species and 615 elementary reactions. Our model has a more accurate residence time than other existing models. This simulation model was verified with industrial data, and the calculation result was highly consistent with the industrial data and more accurate than other approaches. Then, we used this reactor network analysis model to study the effect of the excess air coefficient, the thermal reactor temperature, and the temperature of cooling water on the sulfur recovery efficiency of a real device in the Puguang gas field. The result showed the excess air coefficient and thermal reactor temperature had a clear impact on sulfur recovery efficiency. After analysis, we got the optimum condition parameters for this device. At last, these parameters were tested in the real sulfur recovery device, and the result was reasonable. Our research provides a way to improve the sulfur recovery process in the industry, and it can be helpful to reduce pollution emissions and improve economic performance.

1. Introduction

Sulfur recovery in natural gas extraction has been the subject of much research in the recent years. The Claus process is widely used to recover elementary sulfur from acid gas contained in fresh natural gas. [1] And, the gas from the sour water stripper (SWS) is also a common fuel used in Claus process. It involves thermal oxidation of hydrogen sulfide and its reaction with sulfur dioxide to form sulfur and water vapor.

The basic scheme of a sulfur recovery unit (SRU) is shown in Figure 1. [2] There are five main kinds of devices in the scheme: a burner, a thermal reactor (TR), a waste heat boiler (WHB), two Claus reactors (CR), and a series of sulfur condensers. The acid gas (containing H_2S, CO_2, H_2O, CO, NH_3, and so on) is mixed with air at the burner [3], and then the gas burns and flows into the thermal reactor, which provides necessary residence time to form the Claus gas ($H_2S : SO_2 = 2$). Next, Claus gas goes into the waste heat boiler and the first condenser to cool down, and after that the Claus gas is sent into the Claus reactors.

The two steps of the overall process may be represented as follows. Equation (1) is the overall reaction occurring in the TR. In this process, a third of the total H_2S reacts with oxygen at the best stoichiometric ratio to form Claus gas. The main component of Claus gas is the residual H_2S and the generated SO_2 (the molar concentration ratio of H_2S and SO_2 is about 2, which meets the best stoichiometric ratio of equation (2). Equation (2) takes place in the downstream Claus reactor, and the residual H_2S is oxidized by the generated SO_2 to form S_x. The elemental sulfur is removed by condensation in the three-level condensers:

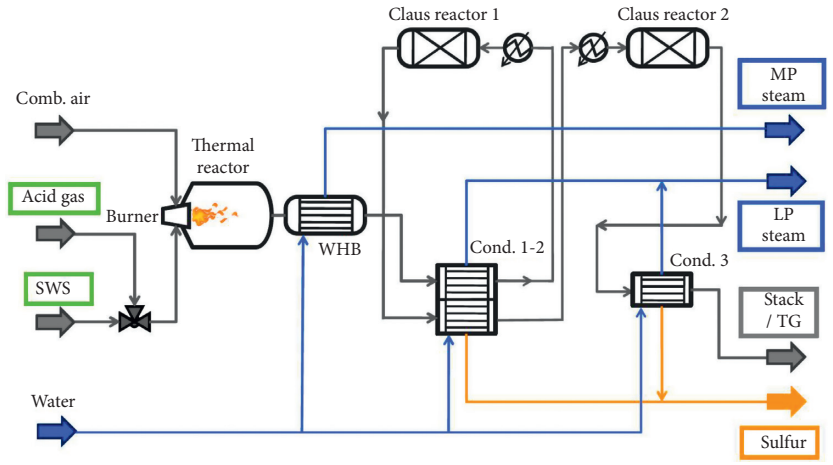

Figure 1: Basic scheme of a sulfur recovery unit.

$$H_2S + \frac{3}{2}O_2 \longrightarrow SO_2 + H_2O \quad (1)$$

$$2H_2S + SO_2 \longrightarrow \frac{3}{2}S_2 + 2H_2O \quad (2)$$

The most efficient and economical way to find the best-operating conditions for an industrial sulfur recovery process is simulation calculation. In 2015, Nabikandi and Fatemi [4] performed a simulation of an industrial Claus SRU process with equilibrium and kinetic methods comparatively. Their research revealed that both kinetic and equilibrium models present reliable results, but the kinetic model which has the ability of prediction compositions, temperature, and pressure along the furnace showed higher potential to cover the industrial results. But, the reaction mechanism in this process is rather complex and has not been completely understood. With the development of the reaction mechanism and the tuning of the kinetic parameters, the kinetic simulation methods can get closer to the real results. After reviewing the kinetic models of H_2S combustion and evaluating the effect of the acid gas impurities, Gupta et al. [5] indicated that a comprehensive kinetic model that can capture the combustion chemistry of H_2S along with the presence of impurities in Claus reactors can improve the efficiency of sulfur recovery processes and sulfur quality. And, the effect of impurities such as aromatics and mercaptans on the Claus process was studied by Ibrahim [6] and Mahdipoor [7], respectively.

Though many industrial simulation studies have been conducted, there is still room for improvement. The authors in [8, 9] built a detailed reaction mechanism of the acid gas, and they used this mechanism to do a CFD simulation of the reactor furnace of the sulfur recovery units which focused on the flow fields of the process. Then, the authors in [3, 10] also did a kinetic simulation of acid gas destruction with a detailed mechanism for simultaneous syngas and sulfur recovery, and their work investigated the optimal operating conditions for H_2 production other than sulfur recovery. Manenti et al. [11–15] did much work on the modeling simulation of the sulfur recovery process, and their work covered not only the revision of the combustion mechanism but also the optimization of the operating conditions for sulfur recovery. Though their work was valuable, the mechanism and model used in their work did not update with the recent research findings. Most of all, their optimization results were not verified by the industrial data.

To find a practical way to improve the efficiency of the industrial sulfur recovery process, this paper was trying to find the optimum operating condition for the sulfur recovery unit, especially for the burner, TR, and WHB. To achieve this, we built a new reactor network analysis (RNA) model with a revised detailed mechanism for the first step. Then, the new analysis model with the revised mechanism was verified with industrial data and other simulation results. After verification, this analysis scheme was used to do the condition optimization research of a real sulfur recovery unit in the Puguang Gas Field in China, and then the calculation result was tested in the factory to see if the optimum parameters work well.

The organization of the paper is as follows. In Section 2, we discuss the development of the reaction mechanism. In Section 3, the settings of the RNA model and the verification of this model are displayed. The operating condition optimization research is provided in Section 4. At last, we made a conclusion of this research in Section 5. The results of this research will provide further data to improve the process of elementary sulfur recovery in the industry, which can be helpful to reduce pollution emissions and improve economic performance.

2. Reaction Mechanism

In our study, we summarized and discussed the recent development of elementary reaction studies at first, and then we selected appropriate reactions to fulfill the reaction mechanism. And, some parameters of certain elementary reactions have been revised according to the new academic results. The final mechanism includes 94 species and 615 elementary reactions.

2.1. H_2S Pyrolysis. H_2S pyrolysis plays a key role in the combustion process; not only because H_2S is the source of the sulfur in SRUs, but also H_2S pyrolysis provides the radical pool, especially in the lean air combustion conditions. In 2003, Binoist et al. [16] did a kinetic study of the pyrolysis of H_2S at different residence times (0.4~1.6 s) and at different temperatures (800~1100°C) by experiment and simulation. A detailed radical mechanism was written to account for the experimental results, and it was in good agreement with the experimental data. According to Binoist et al, the pyrolysis kinetic scheme was the first step and the core of a complete detailed mechanism capable of modeling the various oxidation reactions encountered in an industrial Claus furnace. In 2013, Manenti et al. [2] put forward a revised detailed kinetic scheme for the pyrolysis and oxidation of sulfur compounds. In their research, some adjustments were done to the pyrolysis of H_2S. According to Manenti et al, the kinetic model accuracy was improved by 10–20%, depending on the operating temperature. In 2017, Li et al. [17] presented a detailed kinetic mechanism for describing the chemical process during decomposition of the H_2S–CH_4 mixture under dilution condition, and the prediction of the conversion of H_2S was accurate. The kinetic parameters for the pyrolysis of H_2S are shown in Table 1.

2.2. H_2S Oxidation. In 2013, Zhou et al. [18] studied the oxidation of H_2S in an atmospheric pressure flow reactor at temperatures from 950 to 1150 K, and a comprehensive chemical kinetic model for H_2S was developed. The H_2S oxidation mechanism developed by Zhou et al has been validated versus the experimental data of the diluted H_2S oxidation process. In 2019, Li et al. [19] explored the oxidation mechanisms of H_2S by oxygen on activated carbon, and H_2S adsorbed on activated carbon is oxidized by O_2-producing elemental sulfur, which further oxidized to SO_2. This H_2S oxidation compilation included H_2 oxidation, SO and SO_2 oxidation mechanism, S/H reaction subset, and other significant updated kinetic parameters for the H/S/O system. The reaction path analysis is shown in Figure 2.

In 2016, Barba et al. [20] did an experimental and numerical analysis of the oxidative decomposition of H_2S. In this work, a comprehensive chemical kinetic model for the oxidation of H_2S in a low-oxygen atmosphere was studied, by varying the O_2/H_2S ratio (0.2~0.35), residence time (150~300 ms), and process temperatures (900–1100°C). The results showed a very good agreement with the experimental values at higher temperatures (1100°C). Relevant reactions of the kinetic scheme are shown in Table 2.

2.3. Other Mechanisms

2.3.1. C/H/O Mechanism. The mechanism for C/H/O is taken from the well-known GRI-3.0. This mechanism has been validated by many researchers and experimental results. The data were cited from http://combustion.berkeley.edu/gri-mech/.

Table 1: The kinetic parameters for the pyrolysis of H_2S.

Reactions[a]	A ($cm^3 \cdot mol^{-1} \cdot s^{-1}$)	n	E ($cal \cdot mol^{-1}$)
$S + H + M = SH + M$	0.62×10^{17}	−0.6	0
$S + H_2 = SH + H$	0.14×10^{15}	0.0	19 300
$S_2 + M = S + S + M$	0.48×10^{14}	0.0	77 000
$H + S_2 + M = HS_2 + M$	0.40×10^{14}	2.84	1 665
$SH + SH = S_2 + H_2$	0.50×10^{12}	0.0	0.0
$SH + S = S_2 + H$	0.30×10^{14}	0.0	0.0
$H_2S + M = S + H_2 + M$	0.16×10^{25}	2.613	89 100
$H_2S + H = SH + H_2$	0.35×10^{08}	1.94	904
$H_2S + S = SH + SH$	0.83×10^{14}	0.0	7400
$HS_2 + H = SH + SH$	0.97×10^{08}	1.62	−1030
Duplicate	0.11×10^{14}	0.353	210
$HS_2 + H = S_2 + H_2$	0.12×10^{09}	1.653	−1105
$HS_2 + H = H_2S + S$	0.44×10^{14}	0.0	6326
$HS_2 + S = S_2 + SH$	0.42×10^{07}	2.2	−600
$HS_2 + SH = H_2S + S_2$	0.63×10^{04}	3.050	−1105
$HS_2 + HS_2 = H_2S_2 + S_2$	0.96×10^{1}	1.0	57030
$H_2S_2 + M = SH + SH + M$	0.14×10^{16}	0.0	15 000
$H_2S_2 + H = HS_2 + H_2$	0.50×10^{08}	1.933	−1408
$H_2S_2 + H = H_2S + SH$	0.20×10^{15}	0.0	0.0
$H_2S_2 + S = HS_2 + SH$	0.29×10^{07}	2.31	1204
$H_2S_2 + SH = HS_2 + H_2S$	0.64×10^{04}	2.98	−1480

[a]Declared duplicate reaction.

2.3.2. Formation of Sulfur Vapor (S_2). Thanks to the pyrolysis and oxidation of H_2S, there will be an abundance of S radicals and HS radicals in the thermal reactor. And, elemental sulfur vapor (S_2) can be formed via the following chemical reactions [21]:

$$SH + SH \longleftrightarrow S_2 + H_2 \tag{3}$$

$$M + S + S \longleftrightarrow S_2 + M \tag{4}$$

And, equation (3) leads to the production of H_2, and hydrogen is a species which deserved consideration in the Claus process. As seen in the literature, Cong et al. [8], Ravikumar et al. [10], Savelieva et al. [22], and Li et al. [23] have studied the way to increase hydrogen production via the thermolysis and oxidation of hydrogen sulfide (H_2S).

2.3.3. Molecular Growth of Sulfur. When the concentrations of S, HS, S_2, H_2S_2, and HS_2 are relatively high, the chance of growth from S to S_8 increases. The major steps can be presented as follows [24]:

$$\begin{aligned} S_2 + S + M &\leftrightarrow S_3 + M \\ S_3 + S + M &\leftrightarrow S_4 + M \\ S_4 + S + M &\leftrightarrow S_5\,(c) + M \\ S_5 + S + M &\leftrightarrow S_6\,(c) + M \\ S_6 + S + M &\leftrightarrow S_7\,(c) + M \\ S_7 + S + M &\leftrightarrow S_8\,(c) + M \end{aligned} \tag{5}$$

for thermodynamic reasons, the ring or the cyclic structure of S_5(c) would be formed. Depending on the temperature, an equilibrium would be formed between the open linear

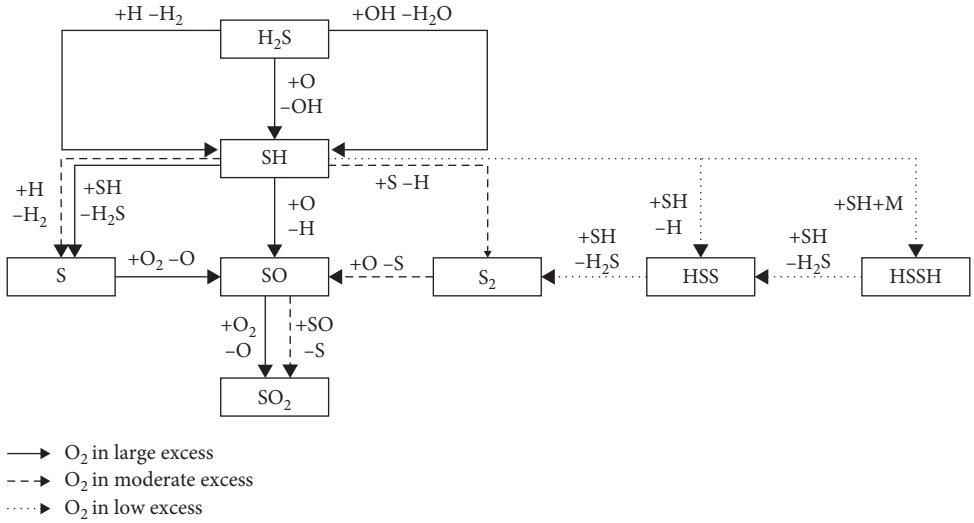

Figure 2: Schematic mechanism for fuel-lean H_2S oxidation showing main consumption pathways.

Table 2: Relevant reactions of the kinetic scheme.

Reactions	A ($cm^3 \cdot mol^{-1} \cdot s^{-1}$)	n	E ($cal \cdot mol^{-1}$)
$S + O_2 = SO + O$	4.898558×10^{05}	2.11	1450.7
$SO + O_2 = SO_2 + O$	7.920000×10^{06}	1.416	3629.0
$H_2O_2 + SH = H_2S + HO_2$	5.570000×10^{04}	2.8	8668.0
$S_2 + O = SO + S$	1.720945×10^{11}	0.7	−231.0
$HS_2 + O_2 = HO_2 + S_2$	4.100000×10^{03}	2.5	10585.0
$SH + O_2 = H + SO_2$	6.500000×10^{11}	0.0	15000.0
$H_2S + S = 2SH$[a]	8.870000×10^{06}	2.3	9007.0
$H_2S + S = 2SH$[a]	9.181582×10^{17}	−1.7	5975.0
$SH + HO_2 = HSO + OH$	2.460000×10^{08}	1.5	−2169.0
$SH + O_2 = SO + OH$	7.500000×10^{04}	2.1	16384.0
$S_2O + SH = HS_2 + SO$	1.000000×10^{13}	0.0	8000.0
$SH + O_2 = HSO + O$	2.290000×10^{06}	1.8	20008.0
$HS_2 + O_2 = HSO + SO$	6.610000×10^{03}	1.9	7071.0

[a]Declared duplicate reaction.

structure and its ring counterpart. [21] The process can be described as the following typical reaction:

$$S_5\,(c) + M \leftrightarrow S_5 + M \tag{6}$$

And, radicals like HS, H_2S_2, and HS_2 can also participate in the formation process of big molecules like S_3~S_8. Typical chemical processes are as follows:

$$S_2 + HS_2 \leftrightarrow S_4 + H \tag{7}$$

$$HS + S_7 \leftrightarrow S_8\,(c) + H \tag{8}$$

2.3.4. Formation of COS and CS_2. There is always CO_2 in the sour gas, and its volume fraction can take up to 40%. The carbon species can react with the sulfur species, and the typical products are carbonyl sulfide (COS) and carbon disulfide (CS_2). In SRUs, COS decreases the production of elemental sulfur and it is a problem for certain Claus catalysts. [13] The chemical paths leading to the formation of those two species involve radical-addition reactions, and the most common mechanism generating COS is as follows:

$$M + CO + S \leftrightarrow COS + M \tag{9}$$

Researchers indicated that the formation of COS has much to do with the presence of CO and sulfur [25–27]. So, we can conclude that CO is the main precursor of COS concerning CO_2. Furthermore, Manenti et al found that CO conversion to COS achieves the thermodynamic equilibrium around 1000°C, which is approximately the typical operating temperature of the thermal reactor furnace where the formation of COS is maximum [13].

A mechanism for the formation of CS_2 is given by Petherbridge et al. [28]. They presented a sequence of reactions leading to the formation of CS_2 as follows:

$$\begin{aligned} SH + CH_3 &\leftrightarrow CH_3SH \\ SH + CH_3 &\leftrightarrow H_2 + CH_2S \\ H + CH_3SH &\leftrightarrow CH_3 + H_2S \\ H + CH_3SH &\leftrightarrow CH_3S + H_2 \\ H + CH_3S &\leftrightarrow CH_2S + H_2 \\ H + CH_2S &\leftrightarrow HCS + H_2 \\ H + HCS &\leftrightarrow H_2 + CS \\ SH + CS &\leftrightarrow H + CS_2 \end{aligned} \tag{10}$$

Their model agreed fairly well with the experimental data, and even experimental errors in the species concentrations have been taken into consideration [21].

2.3.5. The Role of SO_2 in Kinetic Mechanisms. As we can see from the oxidation paths of H_2S, SO_2 is a predominant product. And, SO_2 will take part in the following Claus reaction in the Claus reactor as a major reactant. In the thermal reactor, SO_2 is not likely to be oxidized to SO_3 because of the lack of combustion air. Mueller et al. [29] showed that the increasing concentration of SO_2 progressively decreases the oxidation of CO, highlighting a good agreement between literature data and model predictions.

Dagaut et al. [30] showed that the inhibition effect is progressively reduced with higher temperatures for the cases of stoichiometric and lean inlet oxygen. In the thermal reactor, CS_2 and COS can react with O radicals which were provided by the thermal decomposition of SO_2. The chemical paths are as follows:

$$\begin{aligned} \mathrm{COS + O \leftrightarrow [S - C(O) \equiv O]^* \leftrightarrow CO_2 + S} \\ \mathrm{COS + O \leftrightarrow [O - S - C \equiv O]^* \leftrightarrow CO + SO} \end{aligned} \quad (11)$$

$$\mathrm{CS_2 + O \leftrightarrow [S - C(O) \equiv S]^* \leftrightarrow COS + S} \quad (12)$$

2.3.6. The Oxidation of Methane. In some industrial thermal reactors, CH_4 is used for ignition and to maintain the temperature. The overall scheme for the combustion of methane is well known, and it involves, depending on the conditions, species such as CH_3, CH_2O, CHO, CO, CO_2, C_2H_6, C_2H_4, C_2H_2, CH_2, CH, C_3H_3, and C_6H_6. [31] The two-carbon molecules become more important under fuel-rich conditions. The research by Westbrook and Dryer [32] was meaningful, and they showed that the methane combustion in the atmosphere with hydrogen sulfide under fuel-rich conditions was initiated by

$$\begin{aligned} \mathrm{CH_4 + S \leftrightarrow CH_3 + HS} \\ \mathrm{CH_4 + HS \leftrightarrow CH_3 + H_2S} \end{aligned} \quad (13)$$

Through the above reactions, sulfur species can affect the main chemical paths for methane oxidation.

3. Reactor Network Analysis Model

3.1. Settings of the RNA Model. We used Chemkin Pro to do the analysis, and the scheme of the RNA model is shown in Figure 3. According to Pierucci et al. [33], a perfectly mixed reactor was adopted to describe the mix of acid gas and air. In the model, H_2S was oxidized to SO_2 as soon as it met O_2, while the other species were assumed inert because of the fast ignition of H_2S concerning the other species.

We used a plug flow reactor (PFR) to simulate the thermal reactor by defining the diameter along with the distance. A smaller diameter was used to represent the transition section between the burner and the reactor. Residence time is a key factor influencing the chemical process, and the residence time in this process is more precise in this way.

The acid gas starts to burn at the thermal burner and continues to react in the thermal reactor. Chemical equilibrium is supposed to reach before the outlet of the thermal reactor because of sufficient residence time, so the gas concentration at the end of the thermal reactor is even. The tubes in the waste boiler are the same and independent, so the chemical process and products in different tubes are the same. As a result, a PFR was used to represent one tube in the waste boiler. In the work by Manenti et al. [11, 13], the whole waste boiler was also considered as one tube, so the inlet flow rate and the structure size were not appropriate. In our simulation model, a gas flow splitter (GFS) was used. A certain part of the gas of the thermal reactor was injected into the waste boiler, while the other part of the tail gas was directly transported to the first outlet. The product at this outlet is the same as the product of the thermal reactor. The inlet flow rate of this PFR was calculated according to the number of the tubes in the waste boiler, and the structure size of this PFR was set as the same as the real tube. Through the settings mentioned above, the residence time in the waste boiler was precisely controlled.

For the thermal reactor, the heat transfer can be assumed to be zero because of the adiabatic layer at the outside. For the waste heat boiler, the heat exchange is fierce because of the condensation effect. The tubes in the waste boiler were assumed to be clean, and the heat transfer coefficient was determined only by the heat convection between the gas and the tubes.

3.2. Verification of the RNA Model. A new RNA model with a revised mechanism has been set up according to the introduction above, and before applying this approach, verification was done. The industrial data were adopted from the research by Manenti et al. [15]. The structure parameters and inlet operating conditions are listed in Table 3.

The temperature profile is shown in Figure 4. The value of the temperature at the outlet of WHB is consistent with the industrial data. The temperature in the TR is stable because the layer was adiabatic, and the reaction heat can maintain the temperature. The temperature at the beginning of the WHB has a sharp drop because of the cooling water. The speed of temperature falling decreases with the increase of the reactor length and the residence time because of the decrease in the temperature gradient between the gas and the cooling water.

The gas-phase species composition along the thermal reactor and the waste heat boiler is shown in Figures 5 and 6. Results show that the mole fraction at the beginning of TR changes fiercely and gets to equilibrium long before the exit of the TR. Then in the WHB, the equilibrium and kinetics shift because of the rapid change of temperature. As we can see, the simulation result matches the experimental data very well. The mole fraction of H_2S decreases in the TR because of its oxidation and pyrolysis, while it increases in TR because of the change of chemical equilibrium. The formation of S_2 leads to a sharp rise in mole fraction at the beginning of TR, and then the mole fraction of S_2 decreases sharply in WHB caused by the formation of the sulfur isomers.

Due to the oxidation and pyrolysis of H_2S, the mole fractions of SO_2 and H_2 have a huge increase at the inlet. And, in the WHB, the mole fractions of H_2 and S_2 have a sharp drop, while the mole fraction of H_2S has an equivalent increase because of the shift of the chemical equilibrium. With the continuing falling of temperature in WHB, the mole fractions of most species remain the same except for S_2.

In Manenti et al's work, gas quenching was set at position 7.5 m (corresponding at temperature 950°C) and industrial S_2 data were collected at this position. The mole fraction of S_2 at 7.5 m is 0.0587 which is in accordance with the industrial data (5.9%). After this position, S_2 transforms

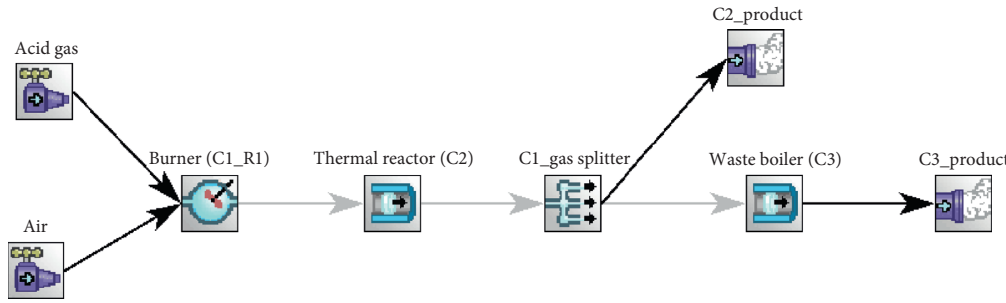

Figure 3: The scheme of the RNA.

Table 3: The structure parameters and inlet operating condition.

Parameters	Value
Acid gas composition (vol %)	C_2H_6 (1.40), CH_4 (2.1), CO_2 (6.62), H_2O (6.40), H_2S (79.55), H_2 (3.7), NH_3 (0.48), C_3H_8 (1.98), CO (0.32), H_2O (6.4)
Acid gas flow rate	4230.5 kg/h
Acid gas temperature	125°C
Combustion air composition (vol %)	H_2O (9.70), N_2 (71.38), O_2 (18.92)
Combustion air flow rate	8907.1 kg/h
Combustion air temperature	45°C
Operating pressure	159 kPa
Reactor length	6.5 m
Reactor diameter	1.55 m
WHB tube length	6.00 m
WHB tube number	470
WHB tube diameter	0.050 m

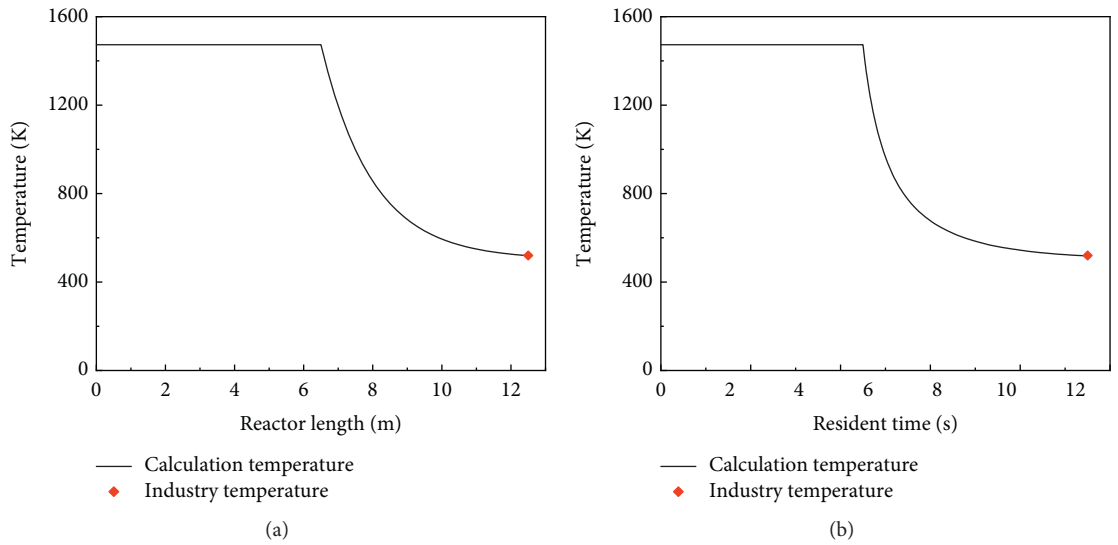

Figure 4: Temperature (K) profile in the TR and WHB.

into other sulfur isomers (shown in Figure 7). There are 8 allotropes (S_1–S_8) of sulfur, and their transition is highly temperature dependent. Among all the isomers, S_2 and S_8 are the most stable ones. S_2 remains stable above 600 K, while S_8 is dominant when the temperature is below this value. As we can conclude from Figure 7, all of the S_2 have converted to other types of sulfur allotropes due to the temperature drop, and the dominant products are S_6, S_7, and S_8.

Based on the calculation result above, we did an error analysis to compare the results between our work and Manenti et al's work (shown in Figure 8). In Figure 8, different colors are used to represent different species and

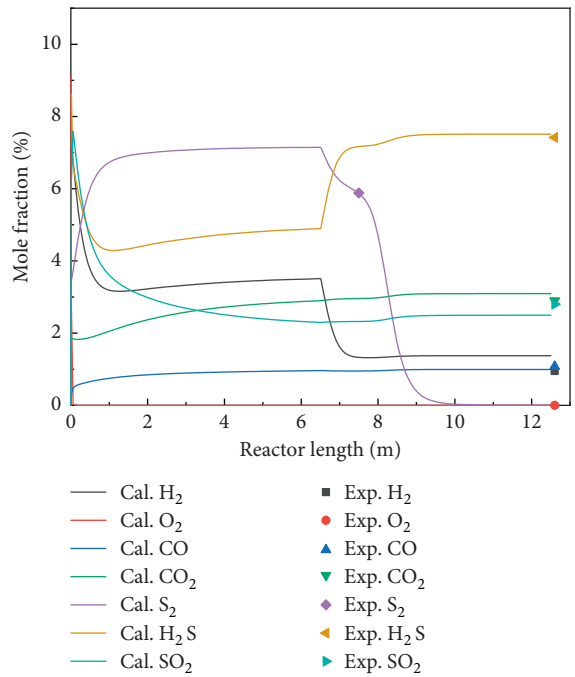

Figure 5: Gas-phase species composition along with the TR and WHB of industrial data and the calculation result.

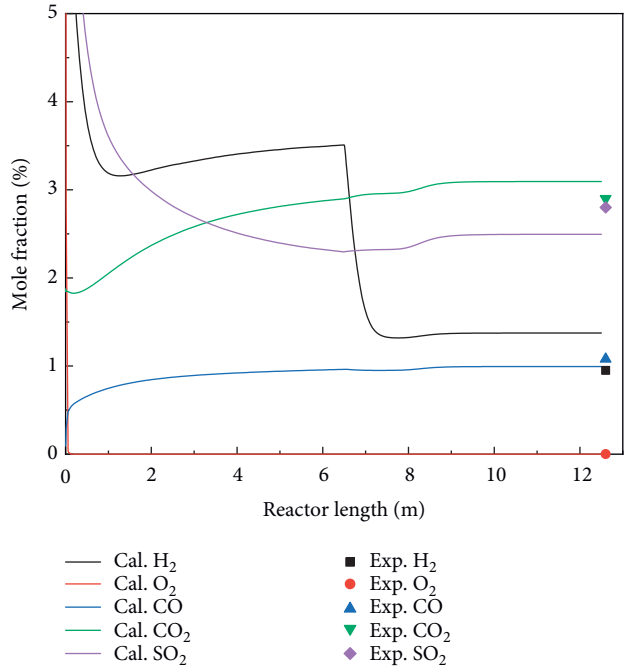

Figure 6: Gas-phase species composition along with the TR and WHB of industrial data and the calculation result (magnified).

squares represent Manenti et al's results while dots represent our results. As we can see, our calculation results have a better prediction in the concentration of all these species except for CO, and the deviations of the CO concentration is acceptable.

Through the analysis above, we can see that the new RNA model with a revised mechanism can not only describe the key features in SRUs but also predict the concentration with good accuracy.

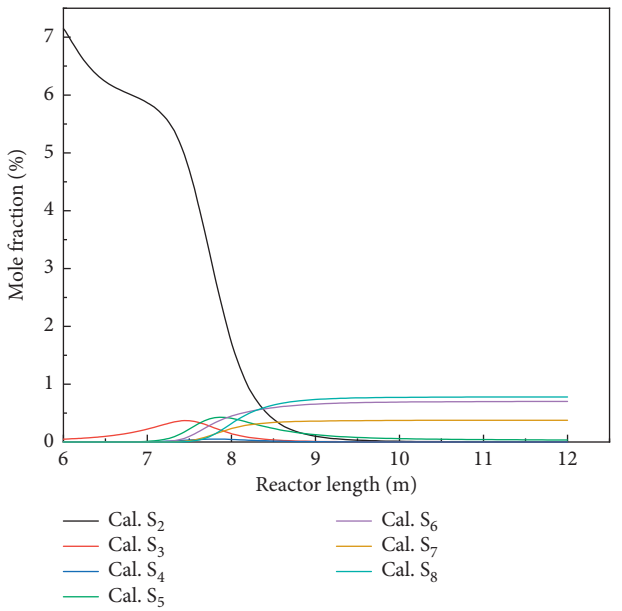

Figure 7: The formation of the sulfur isomers.

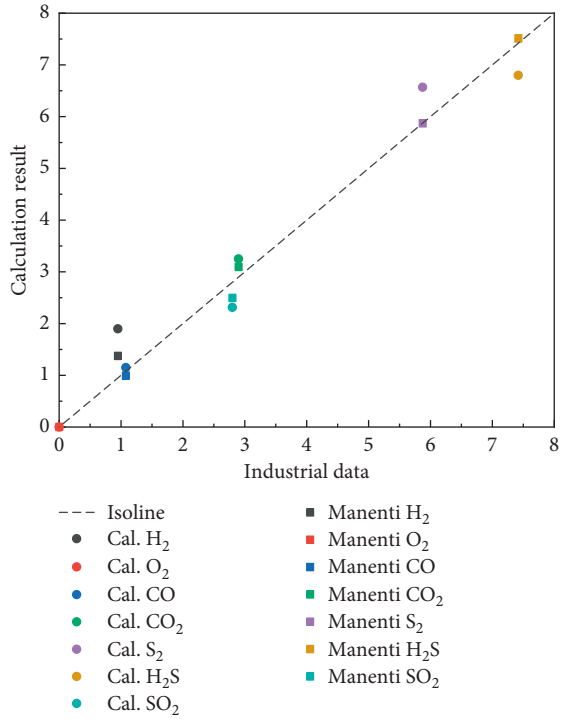

Figure 8: The residuals of the calculated concentration.

4. Optimization Research

4.1. Sulfur Recovery Efficiency. After the verification, we did the parameter optimization study of the burner used in a real factory. This optimization research aimed to obtain the highest sulfur recovery efficiency and in this way will H_2S do

the least harm to the environment. To estimate the H_2S conversion, sulfur recovery efficiency was defined as follows:

$$E_s = \frac{S_{\text{at the exit of SRUs}}}{S_{\text{at the inlet of SRUs}}} = \frac{S_{\text{at the exit of WHB}} + S_{\text{at the exit of CR}}}{S_{\text{at the inlet of SRUs}}}, \tag{14}$$

where E_s stands for the sulfur recovery efficiency and S stands for the total amount of all the allotropes of sulfur, and its unit is g/s. The reaction of H_2S and SO_2 in real CR is always complete, so $S_{\text{at the exit of CR}}$ can be calculated by equation (2) as follows:

$$S_{\text{at the exit of CR}} = \begin{cases} \dfrac{3}{2} \times S_{SO_2 \text{ at the inlet of CR}}, & \left(\text{if } \dfrac{C_{H_2S \text{ at the inlet of CR}}}{C_{SO_2 \text{ at the inlet of CR}}} \geq 2\right), \\ \dfrac{3}{4} \times S_{H_2S \text{ at the inlet of CR}}, & \left(\text{if } \dfrac{C_{H_2S \text{ at the inlet of CR}}}{C_{SO_2 \text{ at the inlet of CR}}} \leq 2\right), \end{cases} \tag{15}$$

where the mass flow rates of SO_2 and H_2S at the inlet of CR are equal to those at the exit of WHB.

4.2. Parameter Optimization Study. In our work, the excess air coefficient, temperature in TR (T_{TR}), and temperature of the cooling water (T_{cw}) were studied. These three parameters can be adjusted easily in the factory. The excess air coefficient and T_{TR} are decided by the amount of fuel and air. The SRUs studied in our paper are located at the Puguang gas field, China. The relating structure parameters and inlet operating conditions are listed in Table 4.

4.2.1. Excess Air Coefficient. The excess air coefficient is controlled by the ratio of acid air to gas. And, from equations (1) and (2), we can see that the best stoichiometric ratio for the complete reaction of H_2S and O_2 is 2. The excess air coefficient is defined as the ratio of the actual amount of air to the amount required for complete combustion of fuel (stoichiometric amount). In a real factory, the excess air coefficient is not always 1 because there are other species in acid gas other than H_2S, taking parting in the subsequent reactions. So, it is useful to find out the best excess air coefficient to gain the highest sulfur recovery efficiency. In this paper, the excess air coefficient varied from 0.7 to 1.4, which means the ratio of the actual amount of air to the stoichiometric amount was from 0.7 to 1.4.

The results are shown in Figure 9. The sulfur recovery efficiency first has an increase and then a decrease with the excess air coefficient varying from 0.7 to 1.4. There is a maximum that lies between 0.9 and 1 where the sulfur recovery efficiency is beyond 95%. This result is reasonable because both too much and too little air will affect the conversion of H_2S. From Figure 9, we can see that the peak point is located near 0.93 and the corresponding sulfur recovery efficiency is beyond 98%.

4.2.2. Temperature in TR. From the verification result, we can see that the concentration of many species changed fiercely near the inlet of the TR. And, after the reactions take place in TR, the gas should contain appropriate H_2S and SO_2. We have reason to believe the temperature in TR is important to the conversion of H_2S. The TR temperature was decided by the amount of fuel. The more the fuel, the higher the TR temperature. The research result of temperature is shown in Figure 10. The sulfur recovery efficiency is not a monotone function of temperature in TR. As the temperature varied from 1073 K to 1473 K, the sulfur recovery efficiency increased clearly at first and then increased with a much slower speed. And at last, it had a significant drop with the increase in temperature. This curve had a peak near 1273 K. This result indicates that the temperature did have a clear influence on the whole sulfur recovery process. Higher temperature means more fuel, and more fuel means more sulfur recovery speed. So, 1273 K was chosen to be the optimum TR temperature in the sulfur recovery process.

4.2.3. Temperature of Cooling Water. From the verification result above, the equilibrium and kinetics in WHB were different from those in TR because of the rapid change of the temperature. So, the change speed of the temperature which is decided by the temperature of the cooling water is important to this process. Different temperatures of the cooling water will result in different WHB outlet temperatures (shown in Figure 11). With the increase of the cooling water temperature, the gas temperature at WHB outlet increased. The lower the cooling water temperature, the more the gas temperature at the WHB outlet dropped with the same residence time and the faster the decrease in the gas temperature in WHB. This result was reasonable. The greater the temperature gradient was, the more powerful the heat transfer was.

The sulfur recovery efficiency as a function of the cooling water temperature is shown in Figure 12. Although the gas temperature at the WHB outlet was influenced by the cooling water temperature obviously, the sulfur recovery efficiency had little reaction to the change of this temperature. With the increase of the cooling water temperature, the sulfur recovery efficiency only had a very slight increase which can be ignored. So, the temperature of the cooling water is always set to the temperature which can help to obtain the highest heat efficiency of the WHB.

Table 4: The structure parameters and inlet operating condition in the Puguang gas field.

Parameters	Value
Acid gas composition (mole %)	CH_4 (0.21), CO_2 (32.28), H_2O (6.97), H_2S (60.52), COS (0.01)
Acid gas flow rate	46827 kg/h
Acid gas temperature	50°C
Combustion air composition (mole %)	H_2O (6.5), N_2 (73.91), O_2 (19.59)
Combustion air flow rate	53530 kg/h
Combustion air temperature	108°C
Operating pressure	159 kPa
Reactor length	6 m
Reactor diameter	2.5 m
WHB tube length	6.00 m
WHB tube number	500
WHB tube diameter	0.074 m

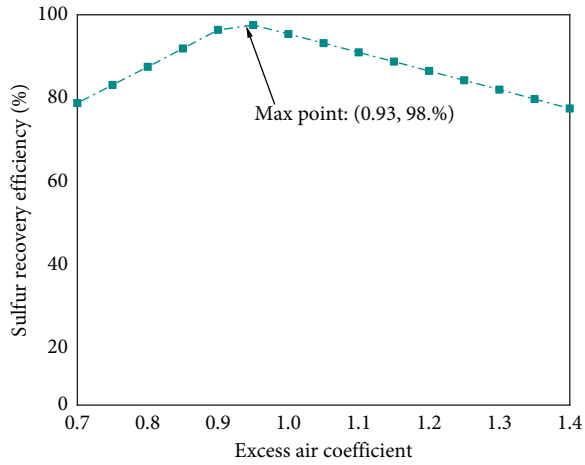

Figure 9: Sulfur recovery efficiency as a function of the excess air coefficient.

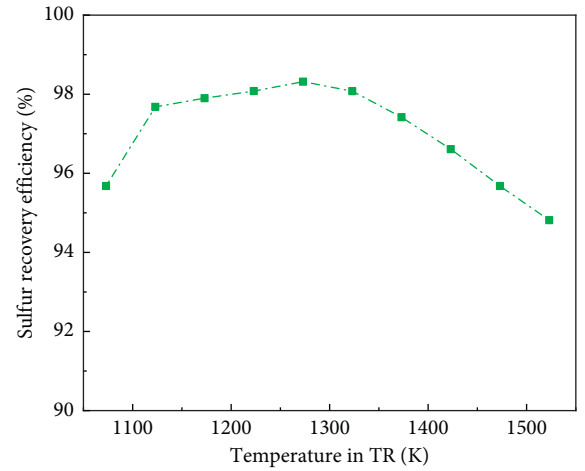

Figure 10: Sulfur recovery efficiency as a function of temperature in TR.

4.3. Test in Factory. Before we tested the calculation result, we recorded an original copy of the industrial data in the Puguang gas field in China. The original operating parameters of SRUs are as follows:

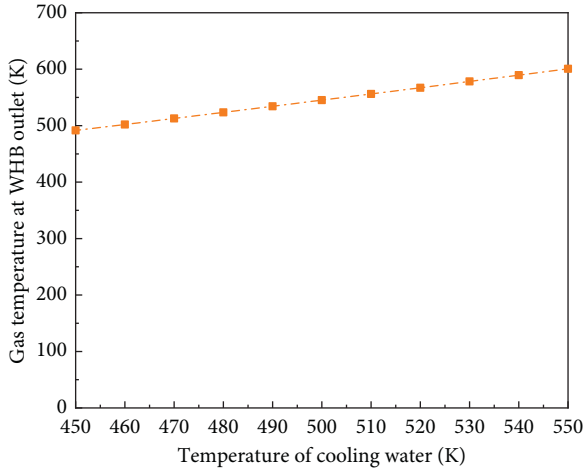

Figure 11: The gas temperature at the WHB outlet as a function of the temperature of cooling water.

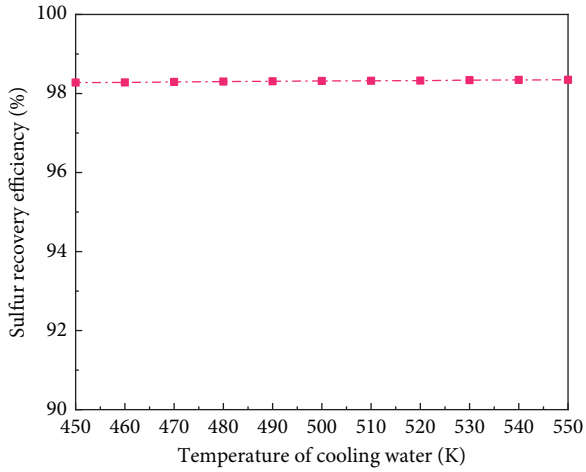

Figure 12: Sulfur recovery efficiency as a function of the temperature of cooling water.

$$Q_{\text{acid gas},1} = 46827\ \text{kg/h}, Q_{\text{air},1} = 53530\ \text{kg/h}, \quad T_{\text{TR},1} = 1270\ \text{K}, \text{ and } T_{\text{CW},1} = 500\ \text{K}. \tag{16}$$

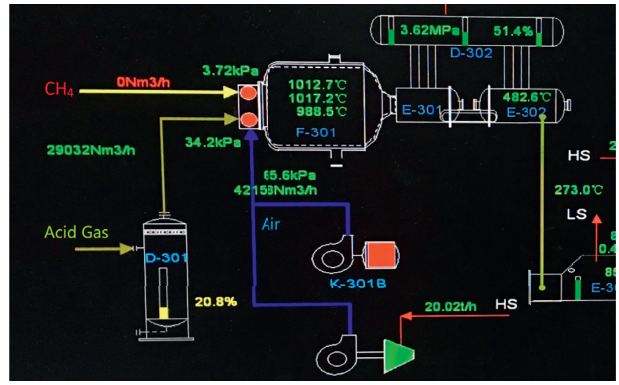

Figure 13: The display screen of the central controller in the Puguang gas field (test situation).

Table 5: Original industrial data and the optimization result.

	Original situation	Optimization situation
Acid gas (kg/s)	13.007	13.007
Air (kg/s)	**14.869**	**14.711**
Excess air coefficient	**0.955**	**0.945**
Temperature in TR (K)	**1270**	**1280**
Temperature of cooling water (K)	500	500
Sulfur production (kg/s)	**6.698**	**6.801**
Sulfur recovery efficiency (%)	**96.07**%	**97.54**%

The sulfur recovery process is a complex industrial process, and it involves so many devices and operations in a real factory that we cannot just simply change the operating parameters as we want. So, after the discussion with the engineers in the factory and considering the optimum operating condition above, the test parameters were as follows:

$$Q_{\text{acid gas},2} = 46827\ \text{kg/h}, Q_{\text{air},2} = 52961\ \text{kg/h}, \quad T_{\text{TR},2} = 1280\ \text{K}, \text{ and } T_{\text{CW},2} = 500\ \text{K}. \tag{17}$$

The flow rate acid gas and the temperature of cooling water in these two situations stayed the same. Figure 13 shows the display screen of the central controller in the Puguang gas field when we tested the optimization parameters. We can see the flow rate of acid gas and air in Figure 13: $Q_{\text{acid gas},1} = Q_{\text{acid gas},2} = 46827\ \text{kg/h} = (46827/36.13) \times 22.4\ \text{Nm}^3/\text{h} = 29032\ \text{Nm}^3/\text{h}$ and $Q_{\text{acid gas},2} = 52961\ \text{kg/}h = (52961/28.14) \times 22.4\ \text{Nm}^3/\text{h} = 42158\ \text{Nm}^3/\text{h}$. And, after calculation, the corresponding excess air coefficient was 0.945.

The comparison of the original situation and test situation is shown in Table 5. The main difference between these two situations was the flow rate of air, which decided the excess air coefficient. The sulfur recovery efficiency in the test situation was higher than that in the original situation, which was consistent with the rules of the effect of the excess air coefficient. In the optimization research, the sulfur recovery efficiency decreased with the excess air coefficient changing from 0.93 to 1.

The test result proved our RNA model was reliable, and it can be a useful tool in the industry. But due to the complexity of the SRUs, we cannot test every possible situation. In our following work, we will improve our RNA model and try to make it capable of investigating the effect of all other parameters. Then, a detailed optimization result will be obtained and tested in the factory.

5. Conclusions

This paper has focused on the optimization of the operating parameters that affect the sulfur recovery efficiency of the SRUs. To get the optimum operating condition, we built a combustion mechanism and a reactor network analysis model to predict the concentration in the Claus process. The calculation results were verified with the industrial data and compared with the work of other researchers. After the verification, the optimization research of real SRUs located in the Puguang gas field was done. Then, the optimum excess air coefficient, temperature in TR, and temperature of the cooling water were obtained. At last, the obtained parameters were tested in the Puguang gas field. Based on the results mentioned above, the following conclusions may be drawn:

(1) The RNA model with the revised mechanism which includes 94 species and 615 elementary reactions had a good predication of the TR and WHB. Because of the more accurate residence time in our model, the calculation results were highly consistent with the industrial data and even more accurate than other researcher's results.

(2) Through the optimization research, we find that the excess air coefficient and the temperature in TR had a clear influence on the sulfur recovery efficiency, while different temperatures of the cooling water

made little difference to the results. After the analysis, the optimum condition parameters were set as follows: excess air coefficient = 0.93, $T_{TR} = 1273^{\circ}K$, and $T_{CW} = 500^{\circ}K$. The corresponding sulfur recovery efficiency was about 98.3%.

(3) The above parameters were tested in real SRUs, and the sulfur recovery efficiency had a clear increase after our optimization research. The whole result had a positive attitude towards the RNA model with the revised mechanism, and it proved that our new approach was a useful tool in the industry.

Data Availability

All data, models, and code generated or used during the study are included within the article.

Conflicts of Interest

The authors declare that they have no conflicts of interest.

Acknowledgments

This study was funded by the National Major Science and Technology Projects of China (2016ZX05017-006), Program for New Century Excellent Talents in University (NCET-13-0468), and Fundamental Research Funds for the Central Universities.

References

[1] R. N. Maddox, *Gas Conditioning and Processing: Gas and Liquid Sweetening*, Campbell Petroleum Series, Oklahoma, OK, USA, 1982.

[2] F. Manenti, D. Papasidero, and E. Ranzi, "Revised kinetic scheme for thermal furnace of sulfur recovery units," *AIDIC Conference Series*, vol. 32, pp. 1185–1290, 2013.

[3] S. Ibrahim and A. Raj, "Kinetic simulation of acid gas (H_2S and CO_2) destruction for simultaneous syngas and sulfur recovery," *Industrial & Engineering Chemistry Research*, vol. 55, no. 24, pp. 132–145, 2016.

[4] N. J. Nabikandi and S. Fatemi, "Kinetic modelling of a commercial sulfur recovery unit based on Claus straight through process: comparison with equilibrium model," *Journal of Industrial & Engineering Chemistry*, vol. 30, pp. 1570–1586, 2015.

[5] A. K. Gupta, S. Ibrahim, and A. Al Shoaibi, "Advances in sulfur chemistry for treatment of acid gases," *Progress in Energy and Combustion Science*, vol. 54, pp. 65–92, 2016.

[6] S. Ibrahim, R. K. Rahman, and A. Raj, "Roles of hydrogen sulfide concentration and fuel gas injection on aromatics emission from claus furnace," *Chemical Engineering Science*, vol. 172, pp. 513–527, 2017.

[7] H. R. Mahdipoor and A. Dehghani Ashkezari, "Feasibility study of a sulfur recovery unit containing mercaptans in lean acid gas feed," *Journal of Natural Gas Science and Engineering*, vol. 31, pp. 585–588, 2016.

[8] T. Y. Cong, A. Raj, J. Chanaphet, S. Mohammed, S. Ibrahim, and A. Al Shoaibi, "A detailed reaction mechanism for hydrogen production via hydrogen sulphide (H_2S) thermolysis and oxidation," *International Journal of Hydrogen Energy*, vol. 41, no. 16, pp. 6662–6675, 2016.

[9] B. Mahmoodi, S. H. Hosseini, G. Ahmadi, and A. Raj, "CFD simulation of reactor furnace of sulfur recovery units by considering kinetics of acid gas (H_2S and CO_2) destruction," *Applied Thermal Engineering*, vol. 123, pp. 699–710, 2017.

[10] A. Ravikumar, A. Raj, S. Ibrahim et al., "Kinetic simulations of H_2 production from H_2S pyrolysis in sulfur recovery units using a detailed reaction mechanism," *Energy & Fuels*, vol. 30, no. 12, 2016.

[11] F. Manenti, D. Papasidero, G. Bozzano, and E. Ranzi, "Model-based optimization of sulfur recovery units," *Computers & Chemical Engineering*, vol. 66, pp. 244–251, 2014.

[12] F. Manenti, D. Papasidero, A. Cuoci et al., "Reactor network analysis of Claus furnace with detailed kinetics," *Computer Aided Chemical Engineering*, vol. 30, pp. 1007–1012, 2012.

[13] F. Manenti, D. Papasidero, A. Frassoldati, G. Bozzano, S. Pierucci, and E. Ranzi, "Multi-scale modeling of Claus thermal furnace and waste heat boiler using detailed kinetics," *Computers & Chemical Engineering*, vol. 59, pp. 219–225, 2013.

[14] F. Manenti, D. Papasidero, and E. Ranzi, "Revised kinetic scheme for thermal furnace of sulfur recovery units," *Chemical Engineering Transactions*, vol. 32, pp. 1285–1290, 2013.

[15] G. Manenti, D. Papasidero, F. Manenti, G. Bozzano, and S. Pierucci, "Design of SRU thermal reactor and waste heat boiler considering recombination reactions," *Procedia Engineering*, vol. 42, pp. 376–383, 2012.

[16] M. Binoist, B. Labégorre, F. Monnet et al., "Kinetic study of the pyrolysis of H_2S," *Industrial & Engineering Chemistry Research*, vol. 42, no. 17, pp. 3943–3951, 2003.

[17] Y. Li, X. Yu, Q. Guo, Z. Dai, G. Yu, and F. Wang, "Kinetic study of decomposition of H_2S and CH_4 for H_2 production using detailed mechanism," *Energy Procedia*, vol. 142, pp. 1065–1070, 2017.

[18] C. Zhou, K. Sendt, and B. S. Haynes, "Experimental and kinetic modelling study of H_2S oxidation," *Proceedings of the Combustion Institute*, vol. 34, no. 1, pp. 625–632, 2013.

[19] Y. Li, Y. Lin, Z. Xu, B. Wang, and T. Zhu, "Oxidation mechanisms of H_2S by oxygen and oxygen-containing functional groups on activated carbon," *Fuel Processing Technology*, vol. 189, pp. 110–119, 2019.

[20] D. Barba, F. Cammarota, V. Vaiano et al., "Experimental and numerical analysis of the oxidative decomposition of H_2S," *Fuel*, vol. 198, pp. 68–75, 2016.

[21] I. A. Gargurevich, "Hydrogen sulfide combustion: relevant issues under claus furnace conditions," *Industrial & Engineering Chemistry Research*, vol. 44, no. 20, pp. 7706–7729, 2005.

[22] V. A. Savelieva, N. S. Titova, and A. M. Starik, "Modeling study of hydrogen production via partial oxidation of H_2S-H_2O blend," *International Journal of Hydrogen Energy*, vol. 42, no. 16, pp. 10854–10866, 2017.

[23] Y. Li, X. Yu, H. Li et al., "Detailed kinetic modeling of homogeneous H_2S-CH_4 oxidation under ultra-rich condition for H_2 production," *Applied Energy*, vol. 208, pp. 905–919, 2017.

[24] A. J. Hynes and P. H. Wine, *Gas-phase Combustion Chemistry: Kinetics and Mechanisms of the Oxidation of Gaseous Sulfur Compounds*, Springer-Verlag, New York, NY, USA, 2000.

[25] M. Abián, M. Cebrián, Á. Millera, R. Bilbao, and M. U. Alzueta, "CS_2 and COS conversion under different combustion conditions," *Combustion and Flame*, vol. 162, no. 5, pp. 2119–2127, 2015.

[26] K. Karan, A. K. Mehrotra, and L. A. Behie, "A high-temperature experimental and modeling study of homogeneous

gas-phase COS reactions applied to claus plants," *Chemical Engineering Science*, vol. 54, no. 15-16, pp. 2999–3006, 1999.

[27] W. D. Monnery, W. Y. Svrcek, and L. A. Behie, "Modelling the modified claus process reaction furnace and the implications on plant design and recovery," *The Canadian Journal of Chemical Engineering*, vol. 71, no. 5, pp. 711–724, 1993.

[28] J. R. Petherbridge, P. W. May, D. E. Shallcross et al., "Simulation of HCS containing gas mixtures relevant to diamond chemical vapour deposition," *Diamond and Related Materials*, vol. 12, no. 12, pp. 2178–2185, 2003.

[29] M. A. Mueller, R. A. Yetter, and F. L. Dryer, "Kinetic modeling of the $CO/H_2O/O_2/NO/SO_2$ system: implications for high-pressure fall-off in the $SO_2 + O\ (+M) = SO_3\ (+M)$ reaction," *International Journal of Chemical Kinetics*, vol. 32, no. 6, pp. 317–339, 2000.

[30] P. Dagaut, F. Lecomte, J. Mieritz, and P. Glarborg, "Experimental and kinetic modeling study of the effect of NO and SO_2 on the oxidation of CO H_2 mixtures," *International Journal of Chemical Kinetics*, vol. 35, no. 11, pp. 564–575, 2003.

[31] J. Warnatz, "Hydrocarbon oxidation high-temperature chemistry," *Pure and Applied Chemistry*, vol. 72, no. 11, pp. 2101–2110, 2000.

[32] C. K. Westbrook and F. L. Dryer, "Chemical kinetic modeling of hydrocarbon combustion," *Progress in Energy and Combustion Science*, vol. 10, no. 1, pp. 1–57, 1984.

[33] S. Pierucci, E. Ranzi, and L. Molinari, "Modeling a claus process reaction furnace via a radical kinetic scheme," *Computer Aided Chemical Engineering*, vol. 18, no. 04, pp. 463–468, 2004.